Hydroelastic response of a submerged structure to an underwater explosion

G. Colicchio[1,2] **M. Greco**[1,2] **O.M. Faltinsen**[2]
giuseppina.colicchio@cnr.it **marilena.greco@cnr.it** **odd.faltinsen@ntnu.no**
1 **CNR-INSEAN, Italian Ship Model Basin, Roma – Italy.**
2 **Centre for Autonomous Marine Operations and Systems (AMOS), Department of Marine Technology, NTNU, Trondheim – Norway.**

The use of composite structures in offshore engineering has revamped the problem of Fluid Structure Interaction (FSI) during underwater blasts because they enhance the FSI effect and increase the shock resistance of underwater structures. The practical applications of these materials range from warfare to offshore infrastructures and to the deep sea fuel transfer installations ([1],[2]). Nonetheless, the techniques that are usually applied to study the FSI rarely make use of the true coupling between the fluid dynamic problem and the structural one.

Most frequently, the hydrodynamic-pressure approximation proposed by Taylor [3] for plates interacting with explosion waves is included in the structural response ([2], [4]). This takes into account the reflected wave pressure and the damping effect due to the absorption of energy from the structure, but it is still a simplified approach. Only for air explosions, the complete coupling is actually modelled ([5],[6]) and only in 1D. Here, taking advantage of the Domain Decomposition strategy outlined in [7], a full 3D FSI investigation is carried out and the computed results highlight the effects of the structural response on the fluid. The differences with the simplified approach are outlined and more quantitative comparisons with available experimental data are underway and will be presented at the workshop.

Description of the problem

The FSI is studied using a 2-DOF structure placed in the path of an incoming spherical blast pressure wave generated by an explosion of a TNT charge as shown in the left panel of figure 1. The pressure wave, generated by the explosion, expands

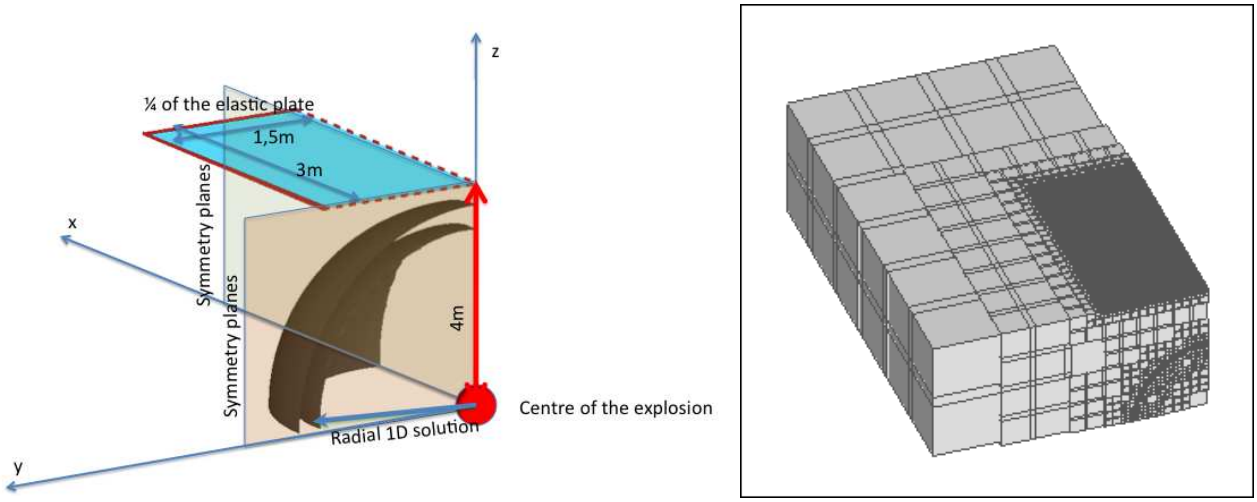

Figure 1: Left: sketch of the problem; a spherical pressure blast is generated by the explosion of a TNT charge positioned at the center of the fluid domain; the pressure wave impacts against an elastic plate. Right: example of the mesh used (the solid lines represent the block boundaries, each block is constituted by 6x6x6 cells.

and touches the upper wall, whose central part, immediately up the charge is constituted of a restrained elastic air-backed orthotropic plate. The symmetry of the problem across the xz and yz planes is used to reduce the computational time. For the same reason an Adaptive Mesh Refinement (AMR) is adopted as shown in the right panel of the same figure. There, the mesh in the fluid is refined close to high pressure gradients and to the plate where the structural and the fluid meshes share the same spacing to avoid numerical interpolations.

Numerical approach

The compressible fluid is described by the equations:

$$\frac{\partial \boldsymbol{U}}{\partial t} + \nabla \cdot \boldsymbol{F} = 0\,, \tag{1}$$

where $\boldsymbol{U} = [u, \rho u, \rho v, \rho w, E]^T$ and $\boldsymbol{F}$ has components $F_x = [\rho u, \rho u^2 + p, \rho uv, \rho uw, (E+p)u]^T$, $F_y = [\rho v, \rho uv, \rho v^2 + p, \rho vw, (E+p)v]^T$ and $F_z = [\rho w, \rho uw, \rho vw, \rho w^2 + p, (E+p)w]^T$. (u, v, w) is the velocity vector, p the pressure, ρ the density and E the total energy $\rho[e + (u^2 + v^2 + w^2)/2]$. The equation of state (EOS) for the specific internal energy e is in the form $\rho e = f_f(\rho)p + g_f(\rho)$,

Equation (1) is solved in an inner region, closer to the explosion center, with a radial approach of the kind:

$$\frac{\partial \boldsymbol{U}}{\partial t} + \frac{\partial \boldsymbol{F}}{\partial r} = \boldsymbol{S}\,, \tag{2}$$

with $\boldsymbol{U} = [\rho, \rho u, E]^T$, $\boldsymbol{F} = [\rho u, \rho u^2 + p, (E+p)u]^T$ and $\boldsymbol{S} = 2[\rho u/r, \rho u^2/r, u(E+p)/r]^T$. This is approximated with a first-order finite-difference scheme in space and time, using the Harten-Lax-Van Leer (HLL) approximated Riemann solver (see [9]).

This solution is coupled to an outer 3D solution of (1) approximated numerically with a second-order finite-difference scheme in space and integrated in time with a Total Variation Diminishing (TVD) third-order Runge-Kutta scheme (see *e.g.* [8]). The fluxes are represented using a Harten-Lax-van Leer contact (HLLC) Riemann solver. It is a modification of the HLL scheme [9] that restores contact and shear waves at the interface and was introduced in [10].

The orthotropic plate, with length L and width B in x and y direction, respectively, is assumed to undergo a linear deformation $\delta(x, y, t)$ governed in time and space by the equation

$$m\frac{\partial^2 \delta}{\partial t^2} + D_x \frac{\partial^4 \delta}{\partial x^4} + 2BB\frac{\partial^4 \delta}{\partial x^2 \partial y^2} + D_y \frac{\partial^4 \delta}{\partial y^4} = p(x, y, \delta, t)\,. \tag{3}$$

Here m is the average plate mass per unit area, D_x and D_y are its flexural rigidities in the two main directions and BB is its effective torsional rigidity (see *e.g.* [11]). $p(x, y, \delta, t)$ is the pressure field calculated from the DD fluid solver.

Fluid structure coupling

A staggered method is used to account for the fluid-structure coupling in time domain. With this method the equation of motion for the plate and the conservation laws for the fluid are alternately integrated in time. The interaction between the fluid and the plate is obtained imposing the continuity of pressure and normal velocity at the structure-fluid interface. Practically, starting at $t = t^n$, when both fluid and structural states are known, the displacement of the structure at $t = t^{n+1}$ is extrapolated from the previous time steps, the fluid is integrated to $t = t^{n+1}$ taking into account the displacement velocity of the plate and the pressure acting on the structure is calculated; the plate configuration is updated to the next time level ($t = t^{n+1}$) using this pressure.

The coupling is forced through the boundary condition on the plate interface for the fluid domain: the vertical velocity w on the fluid-plate interface (fpi) is made symmetric with

$$w_{sym} = -w_{fluid} + 2\dot{\delta} \tag{4}$$

while the pressure is still assumed symmetric across the fpi as for the other boundaries. For the structure, the pressure, calculated in the fluid domain, is immediately available for the forcing term in equation (3). In fact, the mesh used for the fluid solution is exactly superimposed to the one used for the structural calculations. This is the reason for the fine mesh depicted in the right panel of figure 1.

Results

Figure 2 shows the evolution of the pressure wave subsequent to the explosion of a TNT charge causing a gas cavity with initial radius $r_0 = 0.16$ m, density $\rho_{0g} = 1630.0$ Kg/m^3 and pressure $p_{0g} = 8.381 \cdot 10^9$ Pa (see [12] for full information). The isosurfaces $p = 2 \cdot 10^7 N/m^2$ identify the region of high pressure; this region moves out from the centre of the explosion and reaches the plate, 4 m far from the cavity center, at $t \simeq 0.0023s$. At this time instant the pressure on the plate increases abruptly and the plate starts to move upward. The velocity of displacement of the plate (shown with the colored contour level on the right side of each panel) increases slowly and reaches a maximum value of $15m/s$ at the centre of the plate. This value changes very slowly in the last snapshots. The upward movement of the plate causes the generation of a low pressure region at the centre of the plate itself, that sums its effect to the bounce back of the compression wave, leading to a low pressure region that triggers cavitation. Because such phenomenon is not considered in the present model, calculations had to stop at this stage. The bottom right panel of figure 2 shows the comparison for displacement and pressure evolution with and without full FSI coupling. The green lines indicate the evolution with the Taylor assumption for the plate and no feedback of the plate displacement on the fluid. The displacement is larger without FSI; nonetheless the reflection does not give rise to cavitation. The absence of feedback to the fluid prevents also the deformation of the isosurfaces. Their elongation along the main axis of the plate is shown in figure 3. There, the region of

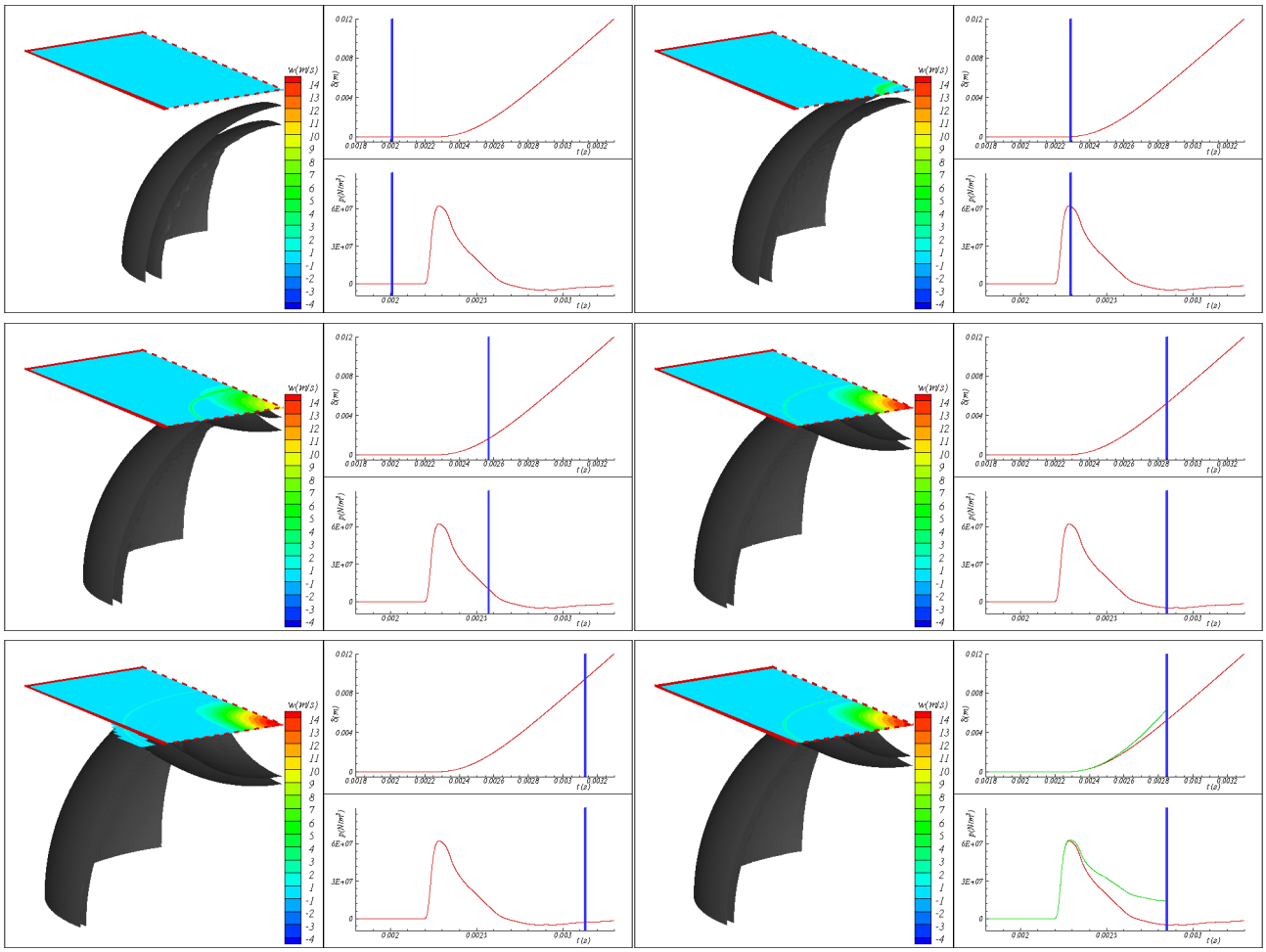

Figure 2: Hydroelastic effects in the FSI investigation. Time increases from left to right and from top to bottom and the time instant is highlighted with a vertical bar in the right plots. For each panel, on the left side: the pressure isosurfaces $p = 2{\cdot}10^7 N/m^2$ and velocity of displacement on the elastic plate; on the top right plot: time evolution of the displacement at the centre of the plate; bottom right plot: pressure acting at the centre of the plate. The most bottom right panel shows comparison of the different pressure and displacement evolution with and without full FSI. Here the pressure is relative to the ambient pressure $p_0 \simeq 0.1$ MPa.

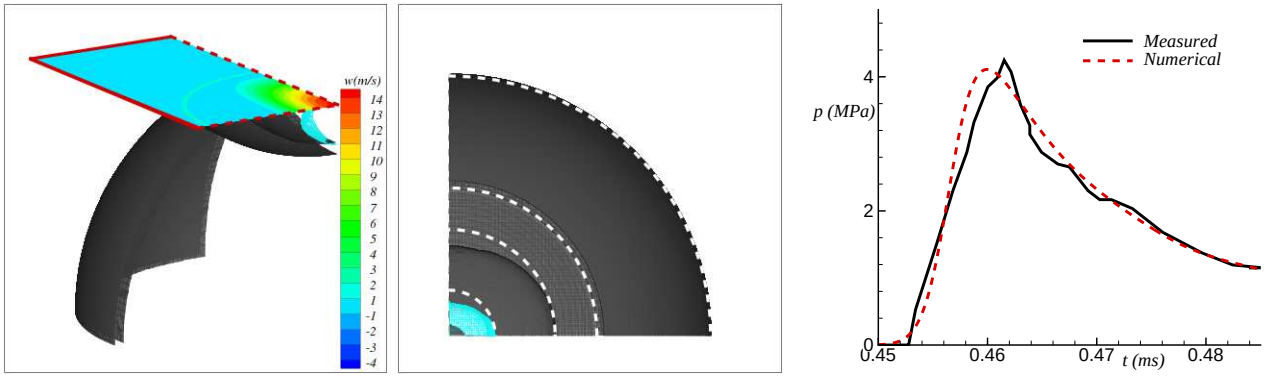

Figure 3: Left and center: 3D effects on the flow field; two different views of the pressure isosurfaces $p = 2 \cdot 10^7 N/m^2$ (dark surfaces) and $p = 0 N/m^2$ (brighter surface). In the centre view, the dashed lines identify the axial-symmetry, the isosurfaces are elongated along the main direction of the plate. Here the pressure is relative to the ambient pressure $p_0 \simeq 0.1$ MPa. Right: underwater explosion in [13]. Comparison of the numerical wave pressure at 0.7m from the explosion, obtained with the radial solver, with the measured time history. Also here p is relative to the ambient pressure in the experiments $p_0 \simeq 0.1$ MPa.

inception of cavitation is given with brighter isosurfaces and the top view (center panel) highlights how all the isosurfaces are elongated along the x direction when compared with the circular traces.

The results shown here lack a validation against experimental results. This is underway and the outcome will be discussed at the workshop, where the solver will be compared with the experimental data from [13] for an air-backed aluminum plate deforming in the elastic regime due to a close-by underwater explosion. Since the used explosive is a combination of a DP60 detonator and a Detasheet and no information is given about initial cavity conditions, the required initial conditions must be identified to properly reproduce the explosion waves interacting with the structure. Right plot of figure 3 provides a preliminary result of the wave pressure at 0.7m from the explosion, corresponding to one of the standoff distance of the plate in the experiments. The curve was obtained by the radial solver assuming an equivalent TNT explosion leading to a cavity with initial radius $r_0 = 0.03$ m, density $\rho_{0g} = 1630.0$ Kg/m^3 and pressure $p_{0g} = 2.1 \cdot 10^{10}$ Pa. The numerical pressure compares fairly well with the measured time history from [13], also shown in the figure, once shifted of 0.018 ms so to synchronize the rising time in the two cases. This means that the numerical explosion is slightly faster than the physical one.

ACKNOWLEDGMENTS

This work was supported partially by the Research Council of Norway through the Centres of Excellence funding scheme AMOS, project number 223254 and partially by the Flagship Project RITMARE - The Italian Research for the Sea - coordinated by the Italian National Research Council and funded by the Italian Ministry of Education, University and Research within the National Research Program 2011-2013.

References

[1] Leblanc J. and Shukla A. Dynamic response of curved composite panels to underwater explosive loading: experimental and computational comparisons. *Composite Structures*, 93 (2011), pp. 30723081

[2] Wang A., Liang X., Fallah A.S., Liu G., Louca L.A. and Wang L. A novel efficient method to evaluate the dynamic response of laminated plates subjected to underwater shock. *Journal of Sound and Vibration* Volume 332, Issue 21, 14 October 2013, Pages 56185634

[3] Taylor G.I., The pressure and impulse of submarine explosion waves on plates *The Scientific Papers of Sir Geoffrey Ingram Taylor*, Cambridge University Press, Cambridge, UK (1963), pp. 287303

[4] Li A., Manolidis M. and Young Y.L. Analytical Modeling of the Underwater Shock Response of Rigid and Elastic Plates Near a Solid Boundary *J. Appl. Mech*. 80(2), 021017 (2013)

[5] Subramaniam K. V., Nian W. and Andreopoulos Y. Blast response simulation of an elastic structure: Evaluation of the fluidstructure interaction effect *International Journal of Impact Engineering* Volume 36, Issue 7, 2009, Pages 965974

[6] Nian, W., Subramaniam, K., and Andreopoulos, Y. Response of an Elastic Structure Subject to Air Shock Considering Fluid-Structure Interaction. *J. Aerosp. Eng.*, 23(3), 176185. 2010.

[7] Colicchio G., Greco M. and Faltinsen O.M. A numerical strategy for gas cavity-body interactions from acoustic to incompressible liquid phases. 28^{th} *Int. Workshop of Water Waves and Floating Bodies.* 2013; pp. 4.

[8] Shu C.W. and Osher S. Efficient implementation of essentially non-oscillatory shock-capturing schemes. *J. Comput. Phys.* 1988; **77**: 439-471.

[9] Toro E.F. *Riemann Solvers and Numerical Methods for Fluid Dynamics.* Springer-Verlag. 1999.

[10] Kim S.D., Lee B.J., Lee H.J. and Jeung I. Robust HLLC Riemann solver with weighted average flux scheme for strong shock. *Journal of Computational Physics*. 2009, **228**: 7634-7642.

[11] Faltinsen O.M. Water entry of a wedge by hydroelastic orthotropic plate theory. *J. Ship Research.* 1999; **43** (3): 180-193.

[12] Smith R.W. AUSM(ALE): A Geometrically Conservative Arbitrary LagrangianEulerian Flux Splitting Scheme. *J. of Computational Physics.* 1999; **150**: 268-286.

[13] Hung C. and Hsu P.Y. and Hwang-Fuu J.J. Elastic shock response of an air-backed plate to underwater explosion. *International Journal of Impact Engineering*, 2005, **31**: 151-168.